

Frequency-domain equalization with interference rejection combining for single carrier multiple-input multiple-output underwater acoustic communications

Jingwei Yin, Wei Ge, Xiao Han, and Longxiang Guo

Citation: [The Journal of the Acoustical Society of America](#) **147**, EL138 (2020); doi: 10.1121/10.0000711

View online: <https://doi.org/10.1121/10.0000711>

View Table of Contents: <https://asa.scitation.org/toc/jas/147/2>

Published by the [Acoustical Society of America](#)

ARTICLES YOU MAY BE INTERESTED IN

[Tracking of multiple surface vessels based on passive acoustic underwater arrays](#)

[The Journal of the Acoustical Society of America](#) **147**, EL87 (2020); <https://doi.org/10.1121/10.0000598>

[Ray-based blind deconvolution of shipping sources using single-snapshot adaptive beamforming](#)

[The Journal of the Acoustical Society of America](#) **147**, EL106 (2020); <https://doi.org/10.1121/10.0000709>

[Broadband low frequency sound absorption using a monostable acoustic metamaterial](#)

[The Journal of the Acoustical Society of America](#) **147**, EL113 (2020); <https://doi.org/10.1121/10.0000714>

[A spatial correlation model for broadband surface noise](#)

[The Journal of the Acoustical Society of America](#) **147**, EL99 (2020); <https://doi.org/10.1121/10.0000710>

[Natural sound estimation in shallow water near shipping lanes](#)

[The Journal of the Acoustical Society of America](#) **147**, EL177 (2020); <https://doi.org/10.1121/10.0000749>

[Machine learning-based classification of recreational fishing vessel kinematics from broadband striation patterns](#)

[The Journal of the Acoustical Society of America](#) **147**, EL184 (2020); <https://doi.org/10.1121/10.0000774>

JASA
THE JOURNAL OF THE
ACOUSTICAL SOCIETY OF AMERICA

Special Issue:
Education in Acoustics

Submit Today!

Frequency-domain equalization with interference rejection combining for single carrier multiple-input multiple-output underwater acoustic communications

Jingwei Yin,^{a)} Wei Ge,^{a)} Xiao Han,^{a),b)} and Longxiang Guo^{a)}

*Acoustic Science and Technology Laboratory, Harbin Engineering University, Harbin 150001, China
yinjingwei@hrbeu.edu.cn, gewei@hrbeu.edu.cn, hanxiao1322@hrbeu.edu.cn, heu503@hrbeu.edu.cn*

Abstract: This paper describes a three-step frequency-domain equalization scheme for multiple-input multiple-output (MIMO) underwater acoustic communication. First, an iterative least-squares channel estimation method is developed to enhance the accuracy of channel estimation in MIMO communication. The interference rejection combining method is then adopted to suppress co-channel interference based on the estimated MIMO channels. This technique exploits the correlation between the interference received through different channels. Finally, a decision feedback equalizer embedded with a digital phase-lock loop is cascaded before the final determination of equalized symbols to compensate the phase rotation. Experimental results show that the bit error rates of the proposed scheme can be several orders of magnitude lower than those of conventional frequency-domain equalization schemes.

© 2020 Acoustical Society of America

[Editor: Charles C. Church]

Pages: EL138–EL143

Received: 29 November 2019 **Accepted:** 19 January 2020 **Published Online:** 12 February 2020

1. Introduction

Multiple-input multiple-output single carrier frequency-domain equalization (MIMO-SC-FDE) is an attractive technique for enhancing underwater acoustic (UWA) communications. However, it faces severe inter-symbol interference (ISI) because of multipath spread, time-varying Doppler effects,¹ and co-channel interference (CoI).^{2,3} In MIMO systems, ISI can be effectively suppressed by using time reversal⁴ and decision feedback equalization (DFE). Multichannel DFE has a lower computational complexity when applied in the frequency domain, a technique referred to as iterative block decision feedback equalization (IB-DFE).⁵ Furthermore, when IB-DFE is integrated with encoding/decoding, it is sometimes called turbo equalization.^{3,6} For time-varying Doppler effects, two suppression methods are common. The first is the second-order digital phase-lock loop (DPLL),⁷ which is often embedded in the time-domain DFE and has been applied in MIMO systems. The second is the group-wise phase correction algorithm proposed by Zheng *et al.*,² which is more robust than DPLL in noisy environments. For CoI in time-domain MIMO-SC systems, Cho *et al.* proposed successive interference cancellation (SIC)⁸ with an adaptive time reversal mirror,⁹ methods that have also been applied to mobile multiuser UWA communications.¹⁰ Song *et al.* proposed parallel interference cancellation (PIC),⁴ which is similar to SIC when multiple iterations are applied. Recently, SIC and PIC have been extended to turbo equalization.^{6,11}

In this paper, a frequency-domain interference rejection combining (IRC) scheme for MIMO-SC systems is proposed. Conventional FDE usually regards the CoI as additive white Gaussian noise (AWGN),^{2,3} but this approach cannot effectively suppress the CoI because this assumption is rarely correct. IRC has been applied to mitigate inter-cell interference in wireless radio communications.^{12,13} Compared with conventional FDE, it exploits the correlation of CoI between different antennas to suppress interference.¹⁴ To improve the accuracy of channel estimation, we propose an iterative least-squares channel estimation (ILS-CE) method with low computational complexity. Although both ISI and CoI can be suppressed effectively by IRC, it cannot deal with the phase rotation caused by time-varying Doppler effects. Therefore, we cascade the DFE embedded with DPLL after the IRC. In this way, the phase rotation can be tracked and compensated and the residual ISI can be further suppressed.

^{a)}Also at: Laboratory of Marine Information Acquisition and Security (Harbin Engineering University), Ministry of Industry and Information Technology, Harbin 150001, China.

^{b)}Author to whom correspondence should be addressed.

2. Signal model

For an SC-MIMO system with N transducers and M hydrophones, the received signal expressed in the frequency domain can be written as

$$Y^m(f) = \sum_{n=1}^N H^{m,n}(f) X^n(f) + Z^m(f), \quad (1)$$

where $H^{m,n}(f)$ is the UWA channel from the n th transducer to the m th hydrophone, $X^n(f)$ is the baseband frequency-domain signal of the n th transducer, and $Z^m(f)$ is the frequency-domain noise. For brevity, f will be omitted from subsequent equations apart from in cases where this may cause confusion. For conventional FDE based on the minimum mean square error (MMSE), the estimation of X^n can be written as

$$X^n = \sum_{m=1}^M \frac{(H^{m,n})^*}{|H^{m,n}|^2 + 1/\gamma} Y^m, \quad (2)$$

where γ is the signal-to-noise ratio (SNR) of the received signal. The conventional FDE assumes that the CoI is AWGN, so the equalization will be performed at a low SNR, for which the performance is obviously not ideal. In addition, CoI does not follow the Gaussian distribution in practice. Simply assuming that the CoI is AWGN does not lead to effective suppression of interference.

3. Frequency-domain receiver

3.1 ILS-CE

Conventional least squares (LS) estimation suffers from some performance degradation in MIMO systems because of the CoI. The basic idea of ILS-CE is shown in Fig. 1. With iterative interference cancellation,^{4,8} the accuracy of the final channel estimation result is greatly improved compared with the initial result in the first iteration. For the first iteration, the frequency-domain form of the received training sequence can be obtained from Eq. (1) as

$$Y_{T1}^m = H^{m,l} X_T^l + \sum_{n \neq l} H^{m,n} X_T^n + Z^m, \quad (3)$$

where Y_T^n is the received training sequence of the m th hydrophone and X_T^n is the expected training sequence of the n th transducer. The initial LS channel estimation results are as follows:

$$\hat{H}_1^{m,l} = Y_{T1}^m (X_T^l)^{-1} = H^{m,l} + E_1^{m,l}, \quad (4)$$

where the channel estimation error is

$$E_1^{m,l} = \sum_{n \neq l} H^{m,n} X_T^n (X_T^l)^{-1} + Z^m (X_T^l)^{-1}. \quad (5)$$

In the second iteration, the interference estimation is carried out first. For the signal transmitted by the l th transducer, the CoI is as follows:

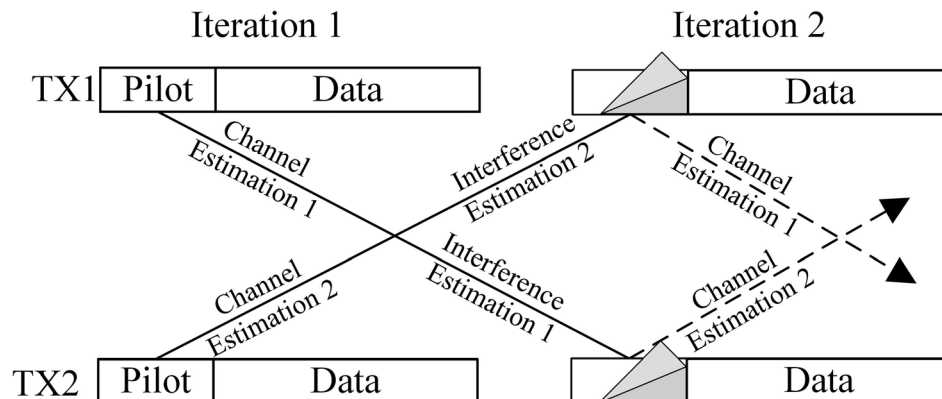


Fig. 1. Schematic of ILS-CE.

$$I_1^{m,l} = \sum_{n \neq l}^N \hat{H}_1^{m,n} X_T^n. \quad (6)$$

The signal after interference cancellation is

$$Y_{T2}^{m,l} = Y_{T1}^m - I_1^{m,l} = H^{m,l} X_T^l - \sum_{n \neq l}^N E_1^{m,n} X_T^n + Z^m. \quad (7)$$

Performing LS channel estimation again gives

$$\hat{H}_2^{m,l} = Y_{T2}^m (X_T^l)^{-1} = H^{m,l} + E_2^{m,l}, \quad (8)$$

where the channel estimation error is

$$E_2^{m,l} = - \sum_{n \neq l}^N E_1^{m,n} X_T^n (X_T^l)^{-1} + Z^m (X_T^l)^{-1}. \quad (9)$$

The mean square error (MSE) is used to measure the accuracy of channel estimation, i.e.,

$$\text{MSE}(\hat{H}) = \frac{1}{f_{\max}} \sum_{f_{\min}}^{f_{\max}} \|H - \hat{H}\|_2^2. \quad (10)$$

When $|\sum_{n \neq l}^N E_1^{m,n} X_T^n|$ in Eq. (9) is less than $|\sum_{n \neq l}^N H^{m,n} X_T^n|$ in Eq. (5), i.e., $|E_2^{m,l}| < |E_1^{m,l}|$,

$$\text{MSE}(\hat{H}_2^{m,l}) < \text{MSE}(\hat{H}_1^{m,l}). \quad (11)$$

Over multiple iterations of interference cancellation, the MSE of the LS channel estimation will continue to decrease, that is, the estimation accuracy will continuously improve.

3.2 Frequency-domain IRC

As the noise received by each array element is uncorrelated, conventional FDE uses the equal ratio combining algorithm to increase the output SNR. However, CoI is typically correlated. The purpose of IRC (Refs. 12 and 13) is to use this correlation to detect and suppress interference. After interference rejection, a higher signal-to-interference-plus-noise ratio (SINR) can be obtained. Figure 2 shows the receiver structure considered in this paper.

MMSE-based IRC. Under the MMSE criterion, the optimal weight vector at a certain frequency for the l th transducer can be written as

$$\mathbf{w}_{\text{opt}}^l = \min_{\mathbf{w}^l} E[|(\mathbf{w}^l)^H \mathbf{Y} - X^l(f)|^2], \quad (12)$$

where $\mathbf{w}^l = [w^{1,l}(f) \ \dots \ w^{m,l}(f) \ \dots \ w^{M,l}(f)]^T$, $\mathbf{Y} = [Y^{1,l}(f) \ \dots \ Y^{m,l}(f) \ \dots \ Y^{M,l}(f)]^T$. $w^{m,l}(f)$ and $Y^{m,l}(f)$ are the weighted vector and received signal of the m th hydrophone from the l th transducer, respectively. The solution of Eq. (12) is

$$\mathbf{w}_{\text{opt}}^l = \frac{\mathbf{H}^l \mathbf{Q}^{-1}}{1 + (\mathbf{H}^l)^H \mathbf{Q}^{-1} \mathbf{H}^l}, \quad (13)$$

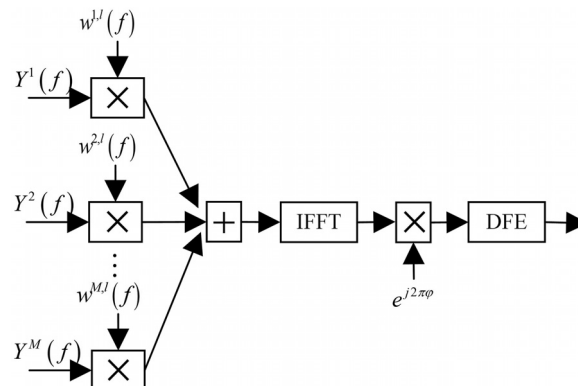


Fig. 2. IRC cascaded with DPLL embedded in DFE.

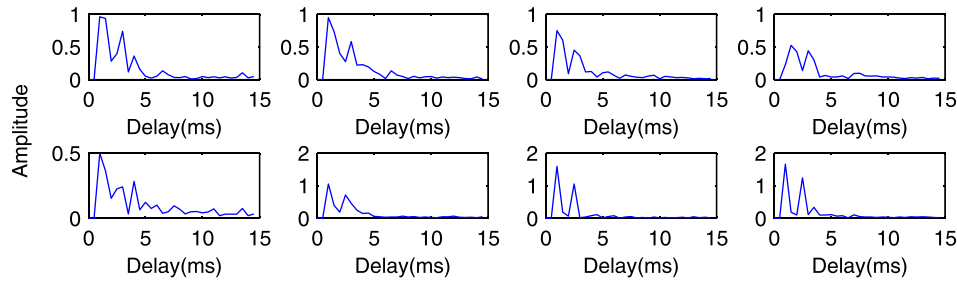


Fig. 3. (Color online) CIRs in the experiment.

where $\mathbf{H}^l = [H^{1,l}(f) \ H^{2,l}(f) \ \dots \ H^{M,l}(f)]^T$. \mathbf{Q} is the covariance matrix of interference noise

$$\mathbf{Q} = \sum_{n \neq l}^N \mathbf{H}^n (\mathbf{H}^n)^H + \sigma^2 \mathbf{I}, \quad (14)$$

where σ^2 is the noise variance and \mathbf{I} is a $M \times M$ matrix.

Maximum signal to interference and noise ratio (MSINR)-based IRC. Define the SINR as follows:

$$\text{SINR} = \frac{E[|(\mathbf{w}^l)^H \mathbf{H}^l X^l(f)|^2]}{E\left[\left|(\mathbf{w}^l)^H \left(\sum_{n \neq l}^N \mathbf{H}^n X^n(f) + \sigma^2 \mathbf{I}\right)\right|^2\right]} = \frac{(\mathbf{w}^l)^H \mathbf{H}^l (\mathbf{H}^l)^H \mathbf{w}^l}{(\mathbf{w}^l)^H \mathbf{Q} \mathbf{w}^l}. \quad (15)$$

The optimum \mathbf{w}^l satisfies the MSINR criterion. To avoid excessive power attenuation of the expected signal, a power limitation is applied, that is,

$$\begin{aligned} \max_{\mathbf{w}^l} & \frac{(\mathbf{w}^l)^H \mathbf{H}^l (\mathbf{H}^l)^H \mathbf{w}^l}{(\mathbf{w}^l)^H \mathbf{Q} \mathbf{w}^l} \\ \text{s.t.} & |(\mathbf{w}^l)^H \mathbf{H}^l| = 1. \end{aligned} \quad (16)$$

The solution of Eq. (16) is

$$\mathbf{w}_{\text{opt}}^l = \frac{\mathbf{Q}^{-1} \mathbf{H}^l}{(\mathbf{H}^l)^H \mathbf{Q}^{-1} \mathbf{H}^l}. \quad (17)$$

Although both ISI and CoI can be suppressed effectively by IRC, phase rotation in fluctuating ocean environments is not effectively mitigated. Therefore, the signal processed in the frequency domain is converted to the time domain using an inverse fast Fourier transform, and then the phase rotation is tracked and compensated by DPLL embedded in DFE to further suppress the residual ISI.

4. Experimental results

A MIMO experiment was carried out in the Bayuquan Sea, off the coast of China. During this experiment, two vertically deployed transducers were used at the transmitter and the data were recorded by a vertical array with four hydrophones. The transmitting transducer spacing was set to 5 m, the top array element was placed 6 m from the water surface, the receiver array element spacing was set to 1.4 m, and the top array element was located 6.5 m from the water surface.

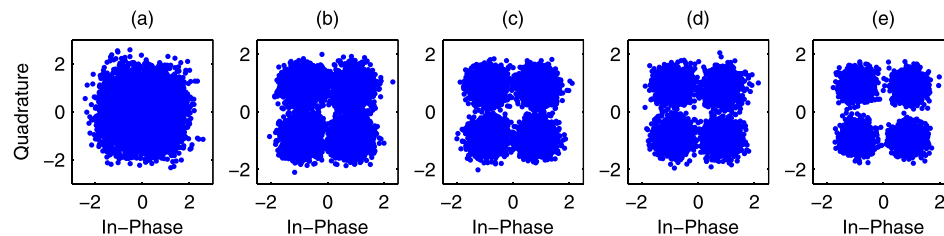


Fig. 4. (Color online) Constellations after equalization with different methods: (a) Conventional FDE equalization, (b) MSINR-based IRC with one-iteration ILS-CE, (c) MMSE-based IRC with one-iteration ILS-CE, (d) MSINR-based IRC with two-iteration ILS-CE, and (e) MMSE-based IRC with two-iteration ILS-CE.

Table 1. BERs after equalization with different methods.

| Data | Con-FDE | MSINR-IRC | MMSE-IRC | Data | Con-FDE | MSINR-IRC | MMSE-IRC |
|------------|---------|-------------------------|----------|------------|---------|-----------|-------------------------|
| BPSK-Iter1 | 0.0845 | 0.0034 | 0.0018 | QPSK-Iter1 | 0.2275 | 0.0073 | 0.0025 |
| BPSK-Iter2 | 0.049 | 1.2207×10^{-4} | 0 | QPSK-Iter2 | 0.2227 | 0.0037 | 7.9423×10^{-4} |
| BPSK-Iter3 | 0.0481 | 1.2207×10^{-4} | 0 | QPSK-Iter3 | 0.2218 | 0.0035 | 7.3314×10^{-4} |

The distance from the transmitter to the receiver was 1 km and the water depth was about 17 m. Quadrature phase-shift keying and binary phase-shift keying (QPSK/BPSK) modulated signals were transmitted in the experiment. The carrier frequency was 10 kHz, the frequency bandwidth ranged from 8 to 12 kHz, and the sampling rate was 96 kHz. Each SC block contained 4096 symbols and 10 ms of zero-padding; 512 symbols at the beginning of each block were used as the training sequence. A recursive LS algorithm was applied in DFE to update the coefficients, with a forgetting factor of 0.9965, feedforward filter span of 10, and feedback filter span of 5.

Figure 3 shows the channel impulse response (CIR) estimated in the experiments. The time-varying Doppler shift was not significant (0.01–0.04 Hz) for the received data. To better verify the performance of the proposed scheme, we added a 1 Hz frequency offset to the received signal, which can be regarded as the Doppler residual after compensation. Figure 4(a) shows the constellation using conventional FDE equalization, in which the phase is blurred and cannot be effectively determined. Figures 4(b) and 4(c) are the constellations using MSINR-based IRC and MMSE-based IRC with one-iteration ILS-CE, respectively. They clearly exhibit a very significant improvement compared with Fig. 4(a). Figures 4(d) and 4(e) show the constellations using MSINR-based IRC and MMSE-based IRC with two-iteration ILS-CE, respectively. The constellations are more separated compared with the results shown in Figs. 4(b) and 4(c).

Table 1 presents the bit error rates (BERs) after equalization by different methods. Using iterative LS estimation, the accuracy of channel estimation can be greatly improved, as reflected by the BER performance. After two iterations, the BER has been greatly reduced and more iterations will not bring about any significant decrease in BER, as most of the interference energy has been removed in the second iteration. Therefore, in order to reduce the computation complexity, two iterations are recommended to implement for practice. The BERs of IRC can be several orders of magnitude lower than that of conventional FDE. In this experiment, MMSE-based IRC performed better than MSINR-based IRC. Figure 5 is the BER curves for Monte Carlo simulation. Similar conclusions as in Table 1 can be obtained under various SNR situations, which verifies the robustness of the method proposed in this letter.

5. Conclusion

This paper has proposed a frequency-domain IRC method for MIMO-SC systems. The experimental results show that multiple iterations of LS channel estimation can significantly improve

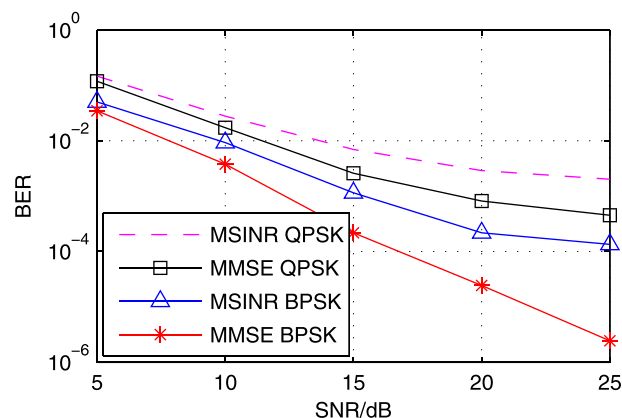


Fig. 5. (Color online) The BER curves after equalization with MSINR- and MMSE-based IRC in Monte Carlo simulation. All the results are based on two-iteration ILS-CE. In the simulation, 100 loops are executed and AWGN is directly added to the received baseband signal after demodulation.

the accuracy of channel estimation. Combining IRC with DFE enables effective mitigation of CoI, ISI, and phase rotation, which is a significant improvement over conventional FDE.

Acknowledgments

This research was funded by the National Natural Science Foundation of China (Grant No. 61631008), the National Key R&D Program of China (Grant No. 2018YFC1405904), the Fok Ying-Tong Education Foundation, China (Grant No. 151007), and the Innovation Special Zone of National Defense Science and Technology and China Scholarship Council.

References and links

- ¹F. Qu, Z. Wang, and L. Yang, "Differential orthogonal space-time block coding modulation for time-variant underwater acoustic channels," *IEEE J. Ocean. Eng.* **42**(1), 188–198 (2016).
- ²J. Zhang and Y. R. Zheng, "Bandwidth-efficient frequency-domain equalization for single carrier multiple-input multiple-output underwater acoustic communications," *J. Acoust. Soc. Am.* **128**(5), 2910–2919 (2010).
- ³Z. Chen, J. Wang, and Y. R. Zheng, "Frequency-domain turbo equalization with iterative channel estimation for MIMO underwater acoustic communications," *IEEE J. Ocean. Eng.* **42**(3), 711–721 (2016).
- ⁴A. Song and M. Badiey, "Time reversal multiple-input/multiple-output acoustic communication enhanced by parallel interference cancellation," *J. Acoust. Soc. Am.* **131**(1), 281–291 (2012).
- ⁵C. He, S. Huo, Q. Zhang, H. Wang, and J. Huang, "Multi-channel iterative FDE for single carrier block transmission over underwater acoustic channels," *China Commun.* **12**(8), 55–61 (2015).
- ⁶J. Tao, J. Wu, Y. R. Zheng, and C. Xiao, "Enhanced MIMO LMMSE turbo equalization: Algorithm, simulations, and undersea experimental results," *IEEE Trans. Signal Process.* **59**(8), 3813–3823 (2011).
- ⁷S. Roy, T. M. Duman, V. McDonald, and J. G. Proakis, "High-rate communication for underwater acoustic channels using multiple transmitters and space-time coding: Receiver structures and experimental results," *IEEE J. Ocean. Eng.* **32**(3), 663–688 (2007).
- ⁸S. E. Cho, H. C. Song, and W. S. Hodgkiss, "Successive interference cancellation for underwater acoustic communications," *IEEE J. Ocean. Eng.* **36**(4), 490–501 (2011).
- ⁹H. Song, J. Kim, W. Hodgkiss, W. Kuperman, and M. Stevenson, "High-rate multiuser communications in shallow water," *J. Acoust. Soc. Am.* **128**(5), 2920–2925 (2010).
- ¹⁰S. Cho, H. Song, and W. Hodgkiss, "Multiuser acoustic communications with mobile users," *J. Acoust. Soc. Am.* **133**(2), 880–890 (2013).
- ¹¹J. Zhang and Y. R. Zheng, "Frequency-domain turbo equalization with soft successive interference cancellation for single carrier MIMO underwater acoustic communications," *IEEE Trans. Wire. Commun.* **10**(9), 2872–2882 (2011).
- ¹²V. Kotzsch, W. Rave, and G. Fettweis, "Interference cancellation and suppression in asynchronous cooperating base station systems," in *IEEE 2012 International ITG Workshop on Smart Antennas (WSA)* (2012), pp. 78–85.
- ¹³C.-C. Cheng, S. Sezginer, H. Sari, and Y. T. Su, "Linear interference suppression with covariance mismatches in MIMO-OFDM systems," *IEEE Trans. Wire. Commun.* **13**(12), 7086–7097 (2014).
- ¹⁴Y. Léost, M. Abdi, R. Richter, and M. Jeschke, "Interference rejection combining in LTE networks," *Bell Labs Tech. J.* **17**(1), 25–49 (2012).